KEK ERL CRYOMODULE DEVELOPMENT

H. Sakai*, T. Furuya, E. Kako, S. Noguchi, M. Sato, S. Sakanaka, T. Shishido, T. Takahashi, K. Umemori, K. Watanabe and Y. Yamamoto
KEK, 1-1, Oho, Tsukuba, Ibaraki, 305-0801, Japan

M. Sawamura
Japan Atomic Energy Agency (JAEA), Tokai, Naka, Ibaraki 319-1195, Japan

K. Shinoe
Institute for Solid State Physics (ISSP), University of Tokyo, Kashiwa, Chiba 277-8581, Japan

Abstract

Development of a SC Cavity Injector Cryomodule and Main linac Cryomodule for the compact ERL (cERL) [1] is being continued at KEK since 2006. Design of an injector cryomodule containing three 2-cell 1.3-GHz cavities for Injector Cryomodule and two 9-cell 1.3-GHz cavities for Main linac Cryomodule are almost completed. Status of R&D and design details are reported.

INJECTOR FOR CERL

An injector for cERL is required to accelerate a CW electron beam of 100mA to 10MeV. In this application, critical hardware components are not cavities but RF input couplers and HOM dampers. Several combinations of number of cavity and cells per cavity were examined, and a three 2-cell cavity system was chosen for cERL. Each cavity is drove by two input couplers to reduce required power handling capacity and also to compensate coupler kick. HOM coupler scheme was chosen for HOM damping, and 5 HOM couplers are put on beam pipes of each cavity. Because of simplicity cavities are cooled by jacket scheme. Basic parameters of the cavity are summarized in Table 1.

Table 1: Basic Cavity Parameters of injector

Frequency	1.3	GHz
Number of cell	2	
R / Q	205	Ω
Operating Gradient	14.5	MV / m
Number of Input Coupler	2	
Coupler Power	167	kW
Coupler Coupling Q	3.3×10^5	
Number of HOM coupler	5	
Operating Temperature	2	k

cavity

A 2-cell cavity is shown in Figure 1. It has a TESLA-like cell shape and larger beam pipe aperture of 88mm. Two fully equipped prototype cavities were fabricated, and the first cold test in a vertical cryostat was done in the last March. The cavity gradient reached 30MV/m with small electron loading (Figure 2). The reason of low Q value is due to losses at beam pipe flanges made of stainless steel. During the test, we observed some thermal instability (blue dots in Fig. 2), where both Q and gradient decrease slowly. It is well known due to the heating of pick-up antennae of HOM couplers. Heating of one HOM coupler was detected by thermometer at around 16 MV/m, but finally we could keep 16 MV/m for 6 hours.

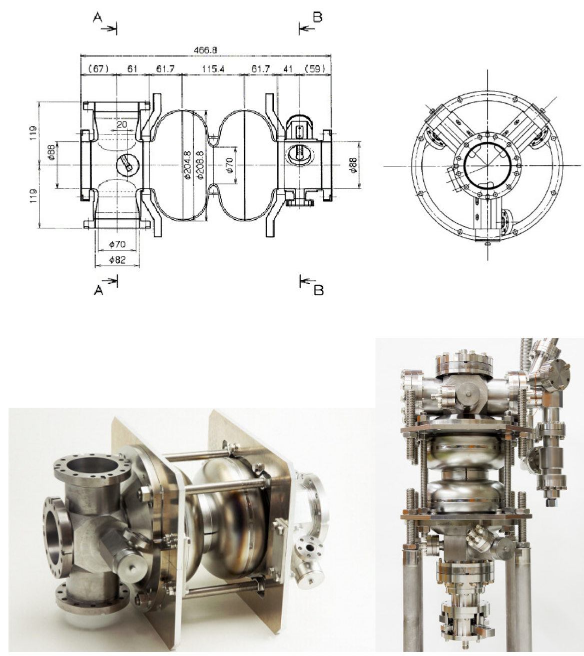

Figure 1: 2-cell Cavity

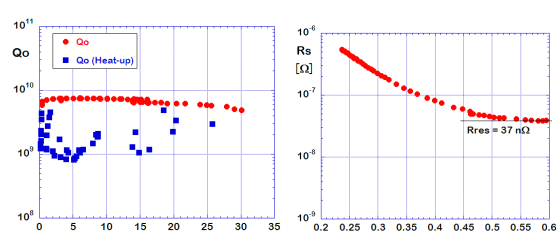

Figure 2: Vertical Test Results.

Input Coupler

RF input coupler is the most critical component in the high power application of the superconducting cavity. The most powerful CW coupler under operation is the KEK-B couplers, which has a coaxial disk type window

* sakai.hiroshi@kek.jp

developed for TRISTAN SC cavities [2]. We made scaled models to 1.3 GHz, as shown in Fig. 3 and 4. Impedance of coaxial part is 41Ω, and the outer diameter is 82 mm.

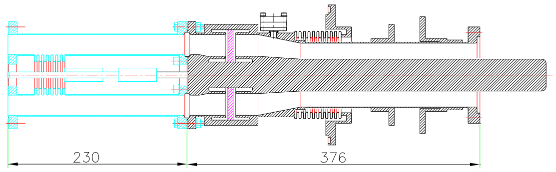

Figure 3: Input Coupler for Injector Cavities.

Couplers will be assembled to cavity in the clean-room before installation to a cryostat, so it should be short as possible. Then thermal intercept becomes difficult, and requires the 5k and 80k anchors at outer conductors. Inner conductors and the windows are cooled by water. High power test is scheduled in September.

Figure 4: Prototype Input Coupler

HOM Coupler

We decided to use HOM couplers instead of beam pipe HOM absorbers to damp HOMs, because absorbers are not well established in cold and they need extra drift space. Major HOMs are summarized in Table 2.

Table 2: Major HOMs

Mode	Frequency	R / Q	Measured Q_L
TE111	1.57GHz	0.59 Ω/cm^2	400
	1.63GHz	1.8 Ω/cm^2	350
TM110	1.80GHz	4.0 Ω/cm^2	1000
	1.88GHz	1.9 Ω/cm^2	900
TM011	2.28GHz	64 Ω	2000
	2.31GHz	12 Ω	1600
TM020	2.67GHz	0.4 Ω	
	2.69GHz	31 Ω	

TESLA HOM couplers are considered as the best choice, but it is well known that thermal instability appears above 10 MV/m in the CW operation. It is also well known that heating happens at pick-up antennae of HOM couplers, but it is not yet understood why niobium antenna becomes normal conducting. One may expect that if the current density at antennae is reduced, the threshold gradient increases. TESLA HOM couplers are modified by introducing second stub and a boss as can be seen in Fig.5 [3].

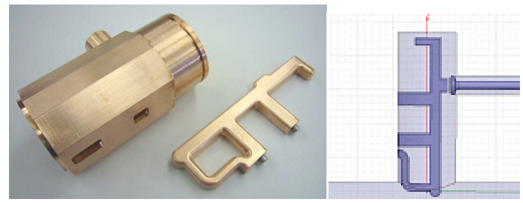

Figure 5: Two Stub HOM Coupler

Fig. 6 shows the H field distribution of the modified HOM coupler, the H field is reduced by a half, to 2000 A/m at 15 MV/m. The first cold test was performed with these HOM couplers. After some processing, we could rise the gradient to 30 MV/m. Heating appeared in one HOM coupler, but we could keep the gradient of 16 MV/m for 6 hours.

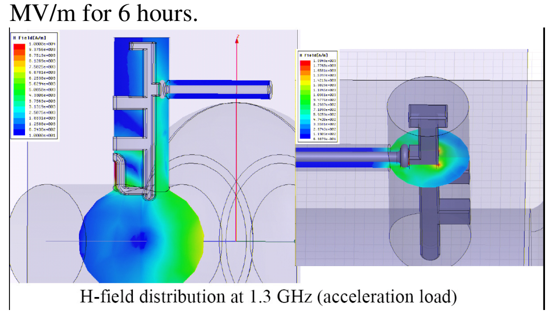

Figure 6: H-Field Distribution

Frequency Tuner

We will use Slide Jack tuners [4, 5] which are used in STF cavities as is shown in Fig. 7. Two pairs of wedge are set on both side of jacket cylinder flanges and driven by one shaft from outside of a cryostat. One piezo system is put in series with a slide jack tuner, and will be replace-able from a cryostat opening. Stroke of the tuner is listed in Table 3.

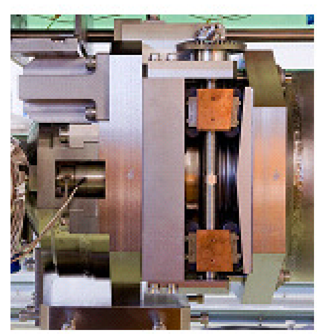

Figure 7: Slide Jack Tuner

Table 3:

	Type	Stroke	Δf
Mechanical Tuner	Slide Jack	1mm	1.3MHz
Fine Tuner	Piezo	4μm	2.6kHz

Cryostat

Fig. 8 and 9 show a cryostat containing three 2-cell cavities. All the cross section may become square. Cavities are dressed with He vessel made of Titanium, and magnetic shields are put inside of He vessel. The estimated cryogenic load in 100mA and 10MV operation is summarized in Table 4. As is seen from this table, it is critical to take dynamic load of input couplers and HOM extraction cables. They will be anchored to 4.5k reservoir panels put on both side of cavities, which works as a thermal shield as well. Because of this difficulty the operating gradient may be lowered.

Table 4: Cryogenic Load per Cavity

	2k		4.5k	
	Static	Dynamic	Static	Dynamic
Cavity	0	6W	0	0
Input Coupler	2W	4W	8W	16W
HOM Cable	1W	7W	5W	14W
Beam Pipe	1W	0	2W	0
Others	5W	0	10W	0
Total	9W	17W	25W	30W

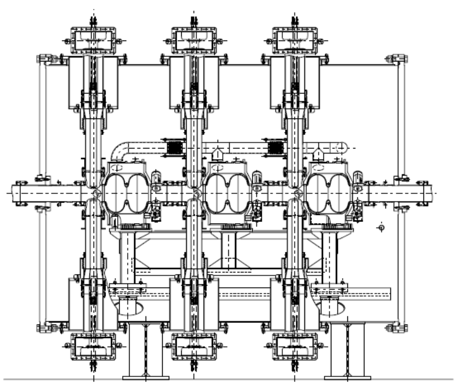

Figure 8: Injector Cryomodule

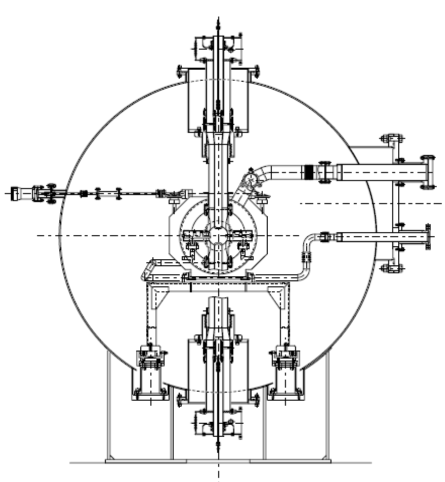

Figure 9: Injector Cryomodule

MAIN LINAC FOR CERL

Nine-cell SC cavities used for the main linac are under development to achieve a stable accelerating gradient of 15 - 20 MV/m under the beam of 100 mA. These cavities were designed [11] so that harmful higher-order-modes (HOMs) can be extracted through large beam pipes to the absorbers set on the 80K temperature. Thanks to the principle of the energy recovery, we can reduce the input power down to 20kW for each cavity. The cavity is cooled down to 2K by using jacket. Basic parameters of the cavity are summarized in Table 5. Because the heat load of HOM absorber is high, the sophisticated cooling is needed for main linac cryomodule.

Table 5: Basic Cavity Parameters of main linac

Frequency	1.3	GHz
Number of cell	9	
R / Q	897	Ω
Operating Gradient	15-20	MV / m
Unloaded Q	$>1 \times 10^{10}$	
Coupler Power	20 (max)	kW
Coupler Coupling Q	$0.5\text{-}2 \times 10^{7}$	
HOM load per HOM absorber	>100	W
Operating Temperature	2	K

cavity

Fig. 10 shows a conceptual view of the KEK-ERL model-2 cavity [6-8], which has been designed for cERL. The TESLA 9-cell cavity was modified to meet our requirements. Its features are the following.

- Cell shape is optimized and large iris diameter of 80 mm is chosen to suppress HOMs.
- Eccentric-fluted beampipe is adopted to suppress quadrupole HOMs.
- HOMs propagate through the large beampipes and are absorbed by HOM absorbers mounted on both sides of the cavity; one is 120mm as Large Beam Pipe (LBP) and the other 100mm as Small Beam Pipe (SBP) .

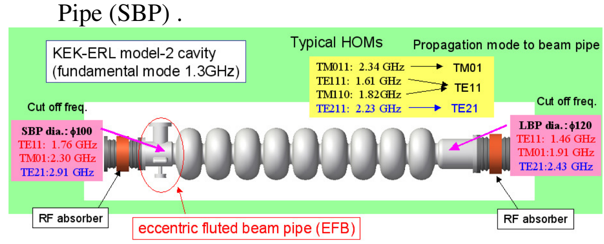

Figure 10: A conceptual view of the KEK-ERL model-2 cavity for the main linac. HOM absorbers are on the both sides.

In order to validate the cavity shape of KEK-ERL model-2, fabrication and surface treatment processes were tested on two single-cell Nb cavities, C-single and E-single, which are shown in the left figures of Fig. 11. C-single has the same cell shape as that of the central cell of the 9-cell structure. E-single has the shape of the end cell equipped with both beam pipes of the 9-cell cavity.

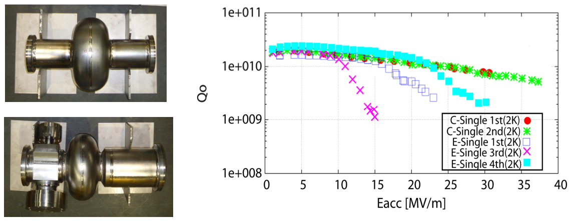

Figure 11: (left)two single-cell cavity one is C-single (top) and another is E-single cavity (bottom). (right) results of the vertical tests of single-cell cavities.

We have first fabricated two Nb single-cell cavities and tested them successfully [9]. The result of vertical tests shows the right figure in Fig.11. C-single and E-single finally satisfied the specification of 20 MV/m with the unloaded-Q of 1×10^{10}. Then, we fabricated a prototype 9-cell cavity, and carried out its vertical tests. The result of vertical tests is shown in Fig. 12. We successfully tested the prototype cavity up to a field gradient of 15 MV/m at 2K, and achieved an unloaded-Q of higher than 10^{10} at 10 MV/m in five vertical measurements. We also observed that the Q-value decreased due to field emissions above the field gradient of 10 MV/m.

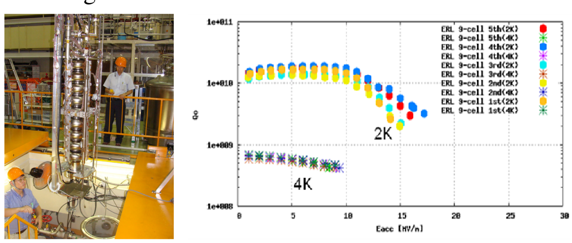

Figure 12: (Left) preparation for the vertical testing the 9-cell cavity. (Right) the first result of the vertical tests.

In order to investigate the cause of this problem in detail, we prepared cavity diagnostics by using rotating mapping system after 4th measurements; one is carbon resistor for measuring heat spot and another is Si PIN diode for measuring X-ray radiation map. Fig.13 shows one of the results of X-ray radiation mapping at 4th vertical measurement. We have strong radiation peak on 8-9 iris around 330° and also see the broad radiation traces on 1-6 irises on 4th and 5th vertical measurements.

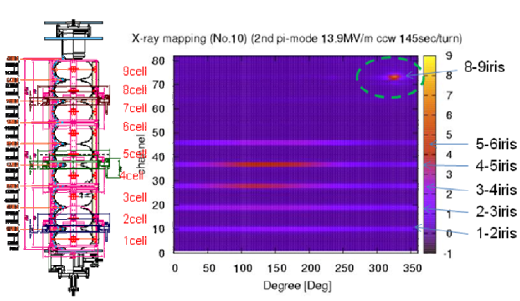

Figure 13: (Left) schematic view of the roating mapping system (Right) the result of radiation mapping.

After 4th and 5th vertical test, we investigate the inner surface by using the optical inspection camera [10]. We found the large tip on 8-9 iris around 150° as shown in Fig.14, which is just opposite side of 330° of the strong radiation point of green dotted circle of Fig.13. From these results, we thing tip of the iris point is one of the radiation sources and it is needed for recovering from field emission to grind this tip.

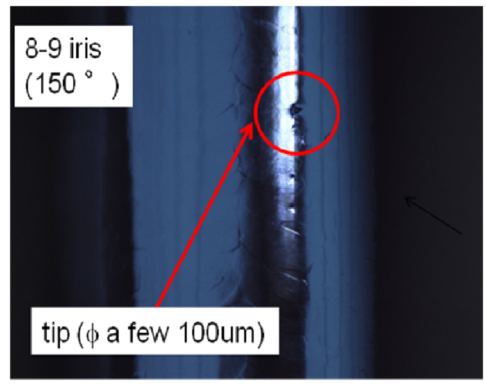

Figure 14: picture of the inner surface on 8-9 iris around 150° by using the optical inspection camera.

Input coupler

Minimum input power is restricted by the cavity detuning due to the microphonics from the cryomodule. We start to consider that the maximum detuning frequency is 50Hz caused by the microphonics. From these results, we determine that the maximum input power is 20kW and loaded Q is 2×10^7 [8].

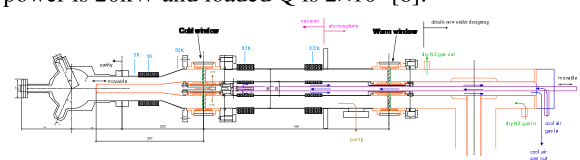

Figure 15: schematic view of input coupler for main linac.

Fig. 15 shows the schematic view of input coupler for main linac. The STF-BL input coupler was modified to meet our requirements [11]. Its features are the following.

- Change the impedance from 50Ω to 60Ω to reduce the heat load of inner conductor. Furthermore forced air cooling was applied to inner conductor.
- Purity of ceramic material was changed from 95%to 99.7% to reduce the heat load of ceramic.
- Cold ceramic size is same as warm one.
- Variable coupling was applied from $Q_L = 5\times10^6$ to 2×10^7 for the short pulse conditioning of input power coupler in commissioning.

In order to check the heat load and temperature of input coupler by feeding the high power, first we made the test stand for testing the components of the input power couplers, especially ceramic windows and bellows, by delivering the maximum 30 kW CW average power from an IOT as shown in Fig. 16.

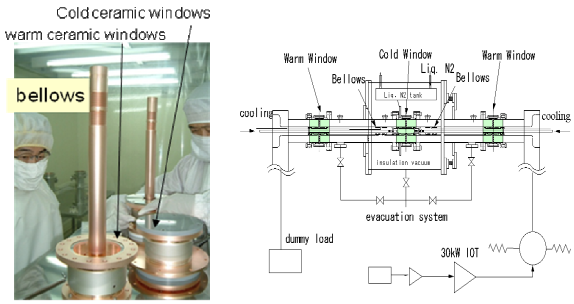

Figure 16: (Left) ceramic windows of input coupler with bellows. (Right) schematic diagram of coupler test stand.

In test stand, warm window with bellows sandwiches the cold window and power go through the 2 warm windows and one cold window. Temperatures of bellows and ceramic windows were monitored. In high power test, the sudden temperature rise was observed when the power increases up to 8kW and finally the cold ceramic window was broken as shown in Fig. 17. In low level test of cold window, we see the sharp resonance peak of 1.305GHz on the S_{21} measurement. And we found this peak is shifted to lower frequency side when temperature is increased. We also found that this frequency is same as the calculation of the unexpected dipole mode which stands on the choke of the ceramic window. From these results, this peak will induce the sudden temperature rise. In order to escape this dipole mode, we plan to modify the ceramic window by changing the thickness of ceramic.

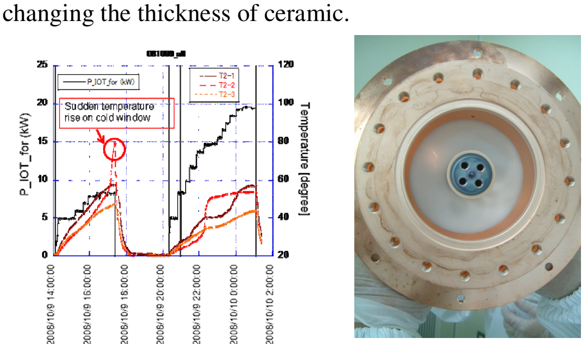

Figure 17: (Left) the measurement of temperature rise of warm ceramic windows (brown, orange line) and cold window (red line) corresponding to the input power (black line). (Right) broken ceramic cold window

HOM absorber

The HOM damper is also important for the ERL. HOM heat load is expected to be more than 100W. Therefore, HOM absorber material is set in the large beam pipes at the temperature of 80K. In order to investigate the enough absorption for high frequency at 80K, we measure the properties of absorption of the 8 kinds of ferrite and one ceramic. The detailed results will be shown in Ref.[12]. After the measurement, we decide to use new-type of IB004, which was used to the HOM absorber of KEKB, for the first prototype of HOM absorber for ERL. Fig.18 shows the design of the prototype of HOM absorber. Its features are the following.

- HIP bonding between ferrite and copper are applied to keep the strong connection
- Comb-type RF bridge is set to suppress the HOM come from the bellows
- Two kinds of thermal anchor at 80K and 5K were applied to absorb the heat load and reduce the static loss from HOM absorber to the cavity.

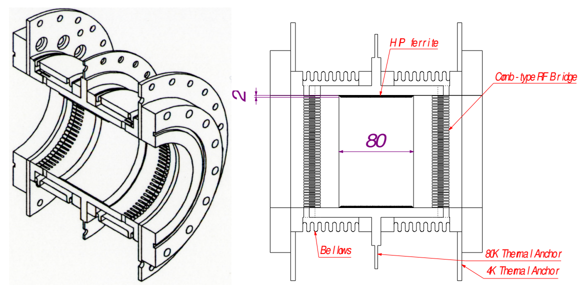

Figure 18: schematic view of HOM absorber

We plan the heat removal test by using this prototype,

Cryostat

Fig. 19 shows the design of the main linac cryomodule containing. Two cavities are set on one cryostat. Cavities are dressed with He vessel made of Titanium, and magnetic shields are put inside of He vessel. We also apply the enlarged jacket size (dia. 300mm) of cavity for smooth pumping of 2K by considering the heat load of 40-50W per cavity. One coupler feeds the RF power to one cavity. Three HOM absorbers set on the cryostat. The dynamic loss come from input coupler and HOM absorber is mainly absorbed 80K thermal anchor and by adding the 5K thermal anchor the static loss is reduced to below 1W to cavities at 2K. We also use the slide tuner to our cavity.

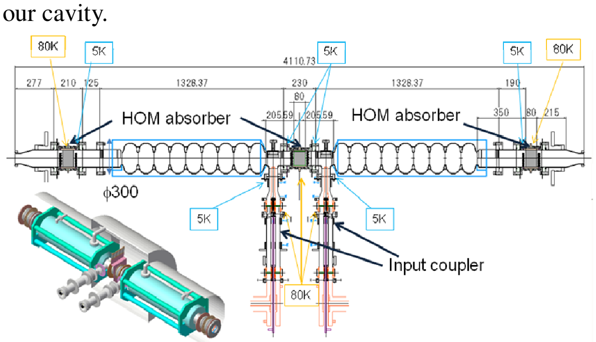

Figure 19: The design of main linac cryomodule.

SUMMARY

Development of Injector and main linac cryomodule are in progress. Assembly of cryomodule is scheduled from 2011 to 2012.

REFERENCES

[1] S. Sakanaka, et al., proc of PAC09, TU5PFP081.
[2] S. Noguchi, et al., "Couplers-Experience at KEK", Proceedings of 4-th SRF Workshop, KEK, 1989, KEK Report 89-21,1990, p.397-p.412.
[3] K. Watanabe, et al., "New HOM coupler Design for ERL Injector at KEK", Proceedings of 13-th SRF Workshop, Peking University, Beijing, China, (2007).
[4] E. Kako, et al., proc. of PAC09, TU3RAI04.
[5] Y. Yamamoto, et al., PAC09, TU5PFP075.
[6] K. Umemori *et al.*, APAC2007, p.570.
[7] M. Sawamura *et al.*, PAC'07, p.1022.
[8] H. Sakai *et al.*, Proc. ERL2007 ,p56
[9] K.Umemori *et al.*, EPAC2008, p.925.
[10] Y. Iwashita et al., Phys. Rev. ST Accel. Beams 11, 093501 (2008).
[11] E.Kako *et al.*,Proc. of the 3rd Annual Meeting Particle Accelerator Society of Japan, Sendai, Japan, 2006, p136.
[12] M.Sawamura *et al.*. in these proceedings of ERL'09